

# A real-time FPGA-based cluster finding algorithm for LHCb silicon pixel detector

Giovanni Bassi<sup>1,2,\*</sup>, Luca Giambastiani<sup>3</sup>, Federico Lazzari<sup>1,4</sup>, Michael J. Morello<sup>1,2</sup>, Tommaso Pajero<sup>5</sup>, and Giovanni Punzi<sup>1,6</sup>

<sup>1</sup>INFN Sezione di Pisa, Pisa, Italy

<sup>2</sup>Scuola Normale Superiore, Pisa, Italy

<sup>3</sup>Università degli Studi di Padova, Padova, Italy

<sup>4</sup>Università degli Studi di Siena, Siena, Italy

<sup>5</sup>University of Oxford, Oxford, United Kingdom

<sup>6</sup>Università di Pisa, Pisa, Italy

**Abstract.** Starting from the next LHC run, the upgraded LHCb High Level Trigger will process events at the full LHC collision rate (averaging 30 MHz). This challenging goal, tackled using a large and heterogeneous computing farm, can be eased addressing lowest-level, more repetitive tasks at the earliest stages of the data acquisition chain. FPGA devices are very well-suited to perform with a high degree of parallelism and efficiency certain computations, that would be significantly demanding if performed on general-purpose architectures. A particularly time-demanding task is the cluster-finding process, due to the 2D pixel geometry of the new LHCb silicon pixel detector. We describe here a custom highly parallel FPGA-based clustering algorithm and its firmware implementation. The algorithm implementation has shown excellent reconstruction quality during qualification tests, while requiring a modest amount of hardware resources. Therefore it can run in the LHCb FPGA readout cards in real time, during data taking at 30 MHz, representing a promising alternative solution to more common CPU-based algorithms.

## 1 Introduction

The LHCb detector [1, 2] is a single-arm forward spectrometer, designed for precision studies of  $b$ - and  $c$ -hadrons produced in  $pp$  collisions. During Run 1 and Run 2, the LHCb detector has shown excellent performance, both in terms of data quality and track reconstruction and particle identification efficiencies. However, one of the main limitations of the current detector is the maximum readout rate (1.1 MHz) of most sub-detectors, constraining trigger efficiencies, particularly in hadronic channels.

To overcome these limitations the LHCb experiment is undergoing an extensive upgrade in view of the upcoming third run of the LHC [3]. Several sub-detectors, including the silicon pixel vertex detector, have been completely redesigned to cope with a peak luminosity  $\mathcal{L} = 2 \times 10^{33} \text{ cm}^{-2} \text{ s}^{-1}$ . A software High Level Trigger (HLT) capable of processing the full inelastic collision rate of 30 MHz is being implemented, improving trigger decision

---

\*e-mail: [giovanni.bassi@cern.ch](mailto:giovanni.bassi@cern.ch)

and maximizing signal efficiencies. The upgraded LHCb data acquisition framework will challenge the whole data handling system due to the large amount of data that has to be processed. In this respect, a common effort is being made to address heavily repetitive tasks at early DAQ stages, leaving to CPUs only the more complex ones. An example of such tasks is the clustering of active pixels in the silicon vertex detector. Grouping contiguous pixels in single hits is both time demanding, due to the 2D pixel geometry, and a highly parallelizable process.

We have developed, implemented and characterized a clustering algorithm that can run on back-end FPGA-based DAQ cards during the detector readout [4, 5]. The features of this algorithm are based on a design developed within the INFN-RETINA R&D project [6].

## 2 Clustering in LHCb pixel detector

The structure of the clustering algorithm is applicable to a general pixel detector, but it has specific features that were tailored for the LHCb Vertex Locator detector (VELO) [7]. VELO detects charged particle in the region closest to the interaction point, aiming at reconstructing primary and secondary vertexes with a spatial resolution smaller than typical decay lengths of *b*- and *c*-hadrons in LHCb ( $c\tau \sim 0.01 - 1$  cm), in order to discriminate between them.

The new VELO, based on silicon pixel technology, will consist of 52 modules positioned along the beam axis, both upstream and downstream of the nominal interaction point. Fig. 1 shows the sub-structure of a VELO layer: a module consists of four sensors, three chips each. A particle crossing a VELO module usually activates more than one pixel. In order to

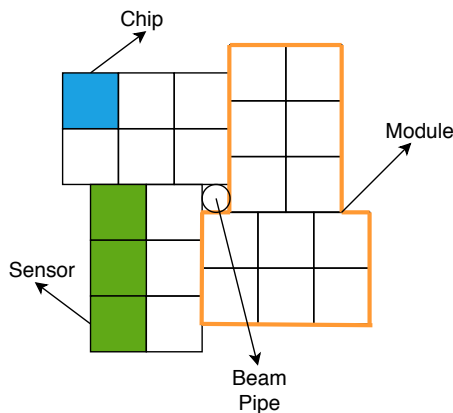


**Figure 1.** Outline of the basic constituents of a VELO layer.

reconstruct the position of the hit, contiguous activated pixels are grouped into clusters.

VELO data are formatted as  $4 \times 2$  pixel blocks, named SuperPixels (SPs). SPs are sorted in two categories, according to the presence of any active neighboring SP: a SP is flagged as ‘isolated’ if none of its eight SP neighbors has any active pixel. This information helps in optimizing the performance of the cluster reconstruction process that follows, allowing a different, faster algorithm for isolated SPs.

## 3 A FPGA-friendly clustering algorithm

Clusters produced by particles hitting the VELO detector typically consist of just few pixels (1-4 pixels in 96% of cases) as shown in Figure 2. For this reason, a significant fraction of

the clusters are isolated, making it convenient to reconstruct them separately with a lookup table (LUT). The LUT is loaded with pre-calculated addresses, linking each of the 256 SP configurations to the cluster coordinates. In this way, reconstructing clusters contained in a single SP requires a very small amount of FPGA resources and is very fast.

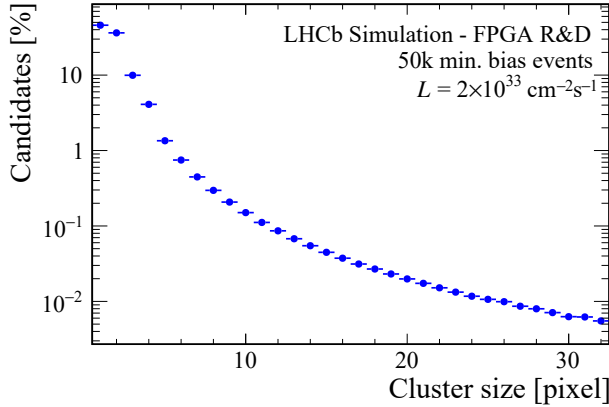


**Figure 2.** Distribution of cluster sizes in 50k simulated minimum-bias events, at the upgrade luminosity.

Finding clusters from not isolated SPs requires a more structured approach, involving multiple steps. For each event, all SPs coming from the same VELO sensor fill a set of matrices, as shown in Fig. 3. Each matrix can contain up to 9 SPs, in three rows and three columns

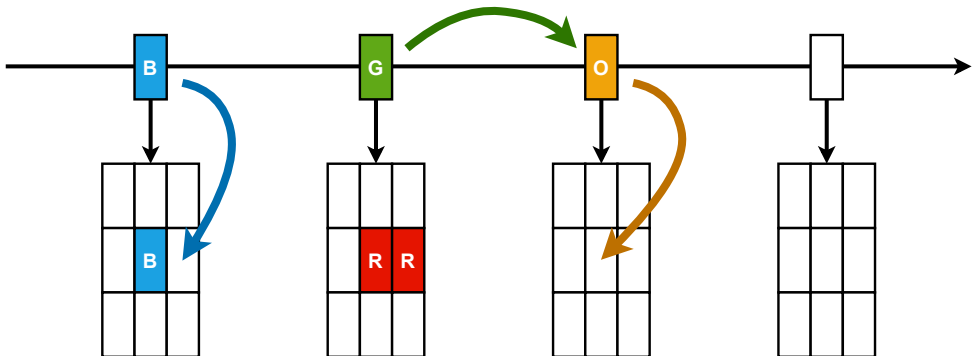


**Figure 3.** Sketch of the matrix filling mechanism with not isolated SPs, coming from a common distribution line. SPs with same color (label) are neighbors. The blue SP (B) in the distribution line belongs to the matrix, it fills it. The green SP (G) does not belong to the matrix, it moves forward. The orange SP (O) has reached an non-initialized matrix, so it is fills the matrix center.

and it does not map to a specific VELO region until it is initialized. As a SP arrives to an uninitialized matrix, it fills the matrix in the center, calculating the coordinates of the neighbouring SPs. Further SPs input to the matrix are compared with the previously calculated coordinates. In case of a match, the pixels status is used to fill the right position in the matrix, otherwise the SPs are passed on to the next matrix in the chain. At the end of each event, in a fully parallel way, each pixel checks if it belongs to one of the patterns shown in Fig. 4.

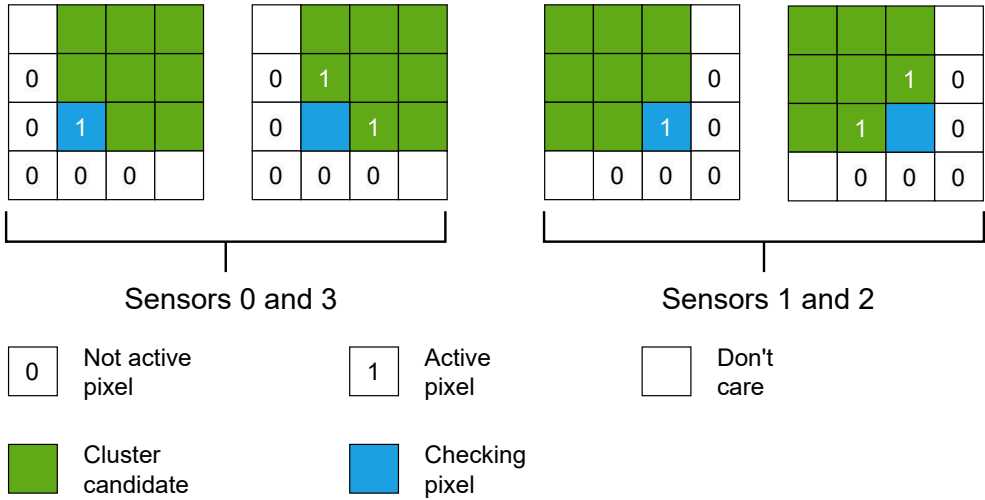


**Figure 4.** Pixel patterns seeding to a cluster candidate. Patterns are optimized for sensor mounting orientation. See [5] for further details.

The corresponding  $3 \times 3$  cluster candidate is then resolved by a LUT. The absolute cluster position is then obtained as a vector sum of the matrix position with respect to the detector, the checking-pixel position with respect to the matrix and cluster position with respect to the checking pixel.

The algorithm has three main parameters that can be optimized. The matrix shape and size are determined by how SPs with neighbors are arranged together, the distribution of the number of SPs with neighbors per event establishes the number of matrices that has to be instantiated. For the VELO clustering algorithm it has been decided to implement 20 matrices for each VELO sensor. The size of the cluster candidates is determined by the distribution of cluster sizes shown in Fig. 2.

## 4 Reconstruction quality

In the FPGA implementation of clustering algorithm, cluster candidates are limited to a  $3 \times 3$  pixel mask. In case of big clusters only a subset of pixels is used in determining the cluster position. Although such clusters are uncommon, clustering and tracking reconstruction quality has been studied to ensure that are not degraded, when FPGA clusters are used. For this purpose, a bit-level simulation of the FPGA clustering algorithm has been implemented and integrated in the official LHCb simulation environment. The HLT tracking is fed with FPGA clusters and its output is compared with that obtained with the standard CPU-based clustering code. The CPU-FPGA comparison has been performed on a 50k minimum-bias simulated event sample, at center of mass energy  $\sqrt{s} = 14$  TeV and luminosity  $\mathcal{L} = 2 \times 10^{33} \text{ cm}^{-2} \text{ s}^{-1}$  (Run 3 upgrade conditions).

Table 1 shows a comparison between CPU- and FPGA-based track reconstruction, for two commonly used LHCb tracks. VELO-tracks are defined to have clusters on three or more VELO layers. T-tracks have at least one x and one stereo cluster in each tracking station downstream the LHCb magnet. If a track is a VELO- and T-track at the same time, then it is a long-track [8]. A clone track is defined to be any additional reconstructed track

matching the same simulated track while a ghost track is a reconstructed track not associated to any simulated track.

Track type	Quantity	CPU cluster	FPGA cluster
VELO tracks	efficiency	98.254% ± 0.007%	98.257% ± 0.007%
	clone	1.231% ± 0.006%	1.233% ± 0.006%
Long tracks	efficiency	99.252% ± 0.006%	99.255% ± 0.006%
	clone	0.806% ± 0.006%	0.807% ± 0.006%
	ghost	0.848% ± 0.003%	0.929% ± 0.003%

**Table 1.** Track reconstruction efficiency, clone and ghost track rates, comparing CPU and FPGA clustering algorithms. Data are 50k minimum-bias simulated events.

Fig. 5 (left) shows a comparison between CPU and FPGA cluster efficiencies as a function of the track pseudorapidity, with a magnified vertical scale to highlight the differences between algorithms. Cluster reconstruction efficiency is defined as the fraction between the number of hits on the detector found by clusters and the number of reconstructible hits. A hit is called reconstructible if the particle generating it has left enough charge in the detector to light up at least one pixel. The overall FPGA cluster inefficiency is below 0.1% within the LHCb geometrical acceptance ( $2 < \eta < 5$ ).

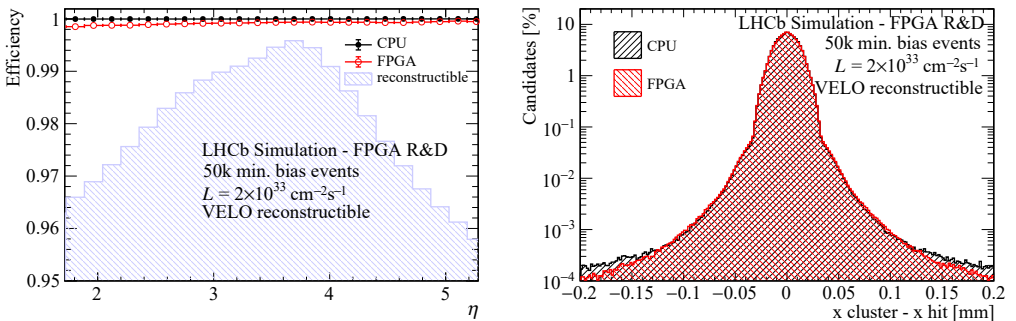


**Figure 5.** Cluster reconstruction quality comparison between CPU and FPGA based clustering algorithms. (Left) cluster reconstruction efficiency as function of the pseudo-rapidity, comparing CPU and FPGA algorithms, within the LHCb acceptance ( $2 < \eta < 5$ ), with a magnified vertical scale to highlight the differences between algorithms. The blue histogram shows the distribution of the detector hits with at least one pixel associated (reconstructible) in pseudo-rapidity. (Right) cluster residual distributions along the x direction, comparing CPU and FPGA clustering algorithms. Only clusters from VELO reconstructible tracks are considered [8]. Data are 50k minimum-bias simulated events.

The quality of the reconstructed clusters is studied using cluster residuals, defined as the distance between the cluster center and the position of the particle associated to it, within the detector. Fig. 5 (right) shows a comparison between CPU and FPGA cluster residual distributions. Differences at the per mille level are observed between CPU and FPGA clustering algorithms for VELO and long track types. These differences have been studied as a function of several kinematic variables. Fig. 6 shows VELO tracking efficiency for long non-electron

tracks, matched to a true simulated particle, as a function of the particle momentum, using CPU and FPGA clusters, with a magnified vertical scale to highlight the differences between algorithms. No significant difference is observed.

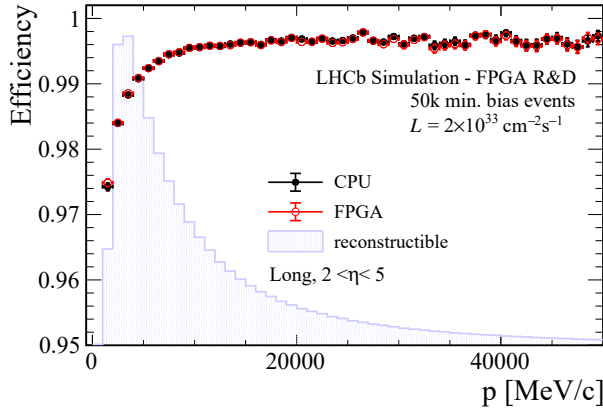


**Figure 6.** VELO tracking efficiency for long non-electron tracks, matched to a true simulated particle, as a function of the particle momentum, comparing CPU and FPGA clustering algorithms. The blue histogram shows the distribution of the particles in momentum. The vertical scale is magnified to highlight the differences between algorithms. Data are 50k minimum-bias simulated events.

## 5 Firmware implementation and hardware testing

The FPGA clustering firmware, available in the public code repository [9], is written in VHDL language, in order to fully exploit the FPGA potential in terms of parallelization, timings, and resources usage. The firmware has a modular structure, where each unit serves a precise purpose [5]. Fig. 7 shows the input-output interfaces, the main components and their connections. Starting from the input side (left side of Fig. 7), a decoding stage splits

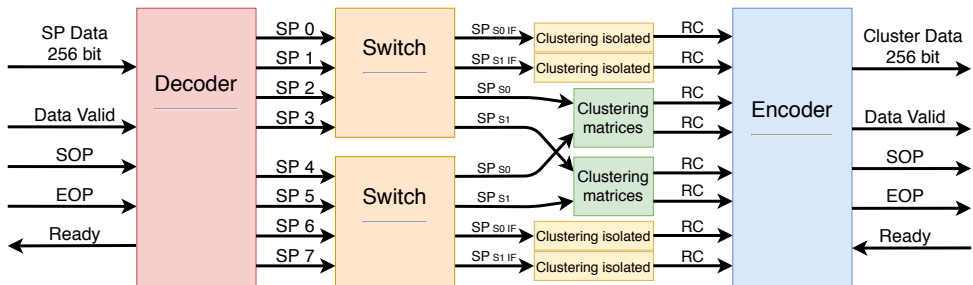


**Figure 7.** Basic blocks of the clustering firmware (SOP: Start Of Package, EOP: End Of Package)

data into separated streams and a switch pair sends data to the appropriate cluster processing blocks. Reconstructed clusters are then encoded back to the appropriate output format. After the developing stage, we tested the firmware on an Intel® Stratix® V based prototyping board [10]. The FPGA used for the test is comparable to the FPGA used on the LHCb DAQ

(Intel® Arria® 10 [11]) in terms of amount of logics and memory. The clustering firmware requires roughly 26% of logics and 10% of memory of an Intel® Arria® 10 chip to process an entire VELO module.

In order to run clustering as a real time process, the firmware has to sustain a 30 MHz event processing rate, to sustain the LHC average bunch crossing rate. The system runs comfortably without errors at a clock frequency of 350 MHz (out of a 650 MHz nominal maximum for our chip model), providing a measured event rate of 38.9 MHz, as shown in Fig. 8, amply sufficient to sustain the target rate of 30 MHz readout.

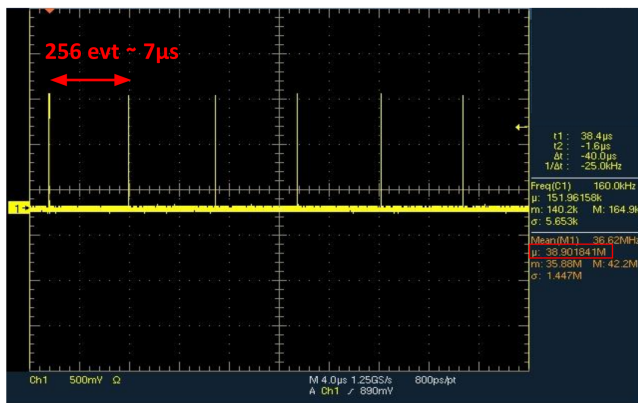


**Figure 8.** Oscilloscope screen shot showing the throughput test result. The FPGA board outputs a signal every 256 events processed.

The firmware, completed with all necessary ancillary logic, has been integrated in the VELO readout firmware as a self-contained block at the end of the processing chain; its output is transmitted out of the readout card via PCIe interface.

A total of 52 Intel® Arria® 10 boards are needed to reconstruct the entire VELO, one board for each module. Even if clustering data from a single VELO module does not require all the FPGA resources available in an Intel® Arria® 10 chip, other operations need to be performed beforehand. Those involve timing-alignment of SuperPixels and SuperPixel flagging tasks [12] that add up to the total amount of resources needed. The resources needed for the entire firmware, from receiving SuperPixels from the detector to cluster reconstruction, are within the FPGA limits so no extra hardware is needed.

## 6 Throughput and bandwidth gains

VELO tracking, including cluster reconstruction, is the most time consuming task of the first stage of the high level trigger (HLT1). It takes about 48% of the HLT1 processing time [13]. Running the HLT1 reconstruction on CPUs with and without the FPGA clustering algorithm shows a gain in the event rate throughput of about 8%. LHCb has recently decided to run the full HLT1 reconstruction on a GPU-based architecture starting from the imminent LHC Run 3 [14]. The GPU-based HLT1 throughput increases by a factor of about 4% offloading VELO clustering to FPGAs. Furthermore, running clustering at early DAQ stages reduces the VELO detector bandwidth [15]. To quantify the reduction, the average number of SPs per event is compared to the corresponding number of reconstructed clusters, leading to a data size reduction of around 15%.

## 7 Summary and outlook

We developed a FPGA-based 2D clustering algorithm for the LHCb silicon pixel detector, capable of processing minimum-bias events at 38.9 MHz. The high processing rate, together with the low amount of FPGA resources required, allows to run the algorithm in real time during the detector readout. The clustering algorithm has been developed to exploit the full flexibility and parallelization potential of FPGAs. The integration within the VELO readout firmware has been carried out, allowing significant throughput and bandwidth gains, thus representing a promising alternative solution to more common CPU-based algorithms, without extra costs. The algorithm physics performance is nearly indistinguishable from CPU clustering and the feasibility of firmware installation in the readout boards has been carefully studied. FPGA clustering is ready to be commissioned for use in physics data taking during Run 3.

## References

- [1] LHCb Collaboration, *JINST* **3**, S08005 (2008)
- [2] LHCb Collaboration, *Int. J. Mod. Phys. A* **30**, 1530022. 73 p (2014)
- [3] LHCb Collaboration, Tech. Rep. [CERN-LHCC-2011-001](#), CERN, Geneva (2011)
- [4] F. Lazzari et al., *J. Phys.: Conf. Ser.* **1525**, 012044 (2020)
- [5] L. Giambastiani, *A 2D FPGA-based clustering algorithm for the LHCb silicon pixel detector running at 30 MHz*, Master's thesis, Università di Pisa, [CERN-THESIS-2020-086](#) (2020)
- [6] R. Cenci et al., *PoS* **313**, 136 (2018)
- [7] LHCb Collaboration, Tech. Rep. [CERN-LHCC-2013-021](#), CERN, Geneva (2013)
- [8] LHCb Collaboration, Tech. Rep. [CERN-LHCC-2014-001](#), CERN, Geneva (2014)
- [9] G. Bassi et al., *FPGA implementation of a fast 2D clustering algorithm (VHDL language)*, INFN Open Access Repository (2019)
- [10] *Dini Group*<sup>®</sup>, <https://www.synopsys.com/verification/prototyping/dini-products.html> (2021), Board model: DNS5GX\_F2, Accessed: 2021-06-28
- [11] *Intel*<sup>®</sup> *Arria*<sup>®</sup> *10 FPGAs*, <https://www.intel.com/content/www/us/en/products/programmable/fpga/arria-10.html> (2021), Accessed: 2021-06-28
- [12] K. Hennessy et al., *Readout firmware of the Vertex Locator for LHCb Run 3 and beyond*, Talk at [22nd Virtual IEEE Real Time Conference](#) (2020)
- [13] LHCb Collaboration, Tech. Rep. [LHCB-FIGURE-2020-007](#), CERN, Geneva (2020)
- [14] LHCb Collaboration, Tech. Rep. [CERN-LHCC-2020-006](#), CERN, Geneva (2020)
- [15] LHCb Collaboration, Tech. Rep. [CERN-LHCC-2014-016](#), CERN, Geneva (2014)